Analytica Chimica Acta 665 (2010) 7–14

Contents lists available at ScienceDirect

Analytica Chimica Acta

journal homepage: www.elsevier.com/locate/aca

A microfluidic approach for anticancer drug analysis based on hydrogel encapsulated tumor cells

Dan Gao[a,b], Jiangjiang Liu[b], Hui-Bin Wei[b], Hai-Fang Li[b], Guang-Sheng Guo[a], Jin-Ming Lin[b,*]

[a] School of Science, Beijing University of Chemical Technology, Beijing 100029, China
[b] The Key Laboratory of Bioorganic Phosphorus Chemistry & Chemical Biology, Department of Chemistry, Tsinghua University, Beijing 100084, China

ARTICLE INFO

Article history:
Received 18 January 2010
Received in revised form 2 March 2010
Accepted 7 March 2010
Available online 12 March 2010

Keywords:
Microfluidic device
Hydrogel microstructures
Cell encapsulation
Anticancer drug

ABSTRACT

A novel method based on fluorescence detection of hydrogel encapsulated cells in microchannels was developed for anticancer drug analysis. In this work, human hepatoma HepG2 cells and human lung epithelial A549 cells were simultaneously immobilized inside two different shapes of three-dimensional hydrogel microstructures using photolithography approach on a same array. Microarrays of living cells offer the potential for parallel detection of many cells and thereby enable high-throughput assays. Using a photolithographic setup, we investigated the prepolymer composition and crosslinking parameters that influenced cell viability inside photocrosslinked hydrogels. The viability of cells encapsulated inside hydrogel microstructures was higher than 90% under optimized photocrosslinking conditions. The cells were further cultured under stable conditions and remained viable for at least three days that were able to carry out cell-based assays. Furthermore, we studied the variation of two intracellular redox parameters (glutathione and reactive oxygen species) in anticancer drug-induced apoptosis in HepG2 and A549 cells. Two anticancer drugs exhibited distinct effects on the levels of intracellular glutathione and reactive oxygen species, indicating the selectivity of these drugs on the disturbance of redox balance within cells. The established platform provides a convenient and fast method for monitoring the effect of anticancer drugs on tumor cells, which is very useful for fundamental biomedical research.

1. Introduction

Functional cell-based assays are becoming an important in postgenomic biomedical research and anticancer therapies [1]. Evaluation of cell response to anticancer agents is an important issue in the therapy of cancers. As different modes of cancer cell death can be induced by efficacious anticancer treatment, accurate detection of apoptotic events is of utmost importance in preclinical drug screening procedures [2,3]. The early diagnosis of cancers is also important because it can reduce chemotherapeutic side effects by using lower doses of drugs. Common cancer therapies, including radiation, chemotherapy, immunotherapy, and gene therapy, aims to reduce or eliminate cancer cells to cure cancer. However, these methods for the analysis of apoptotic events are limited by low assay throughput and tedious sample pretreatment. Consequently, there is a strong need for the development of methods to solve those problems.

Microfluidic devices offer several advantages for cell-based assays, such as minimal reagent consumption, flexible manipulation, large-scale integration and fast analysis time [4]. The dimensions of microfluidic channels are suitable for cell introduction, manipulation, reaction, separation and detection. Most importantly, the microchannels within the microfluidic devices can mimic the physical environment in vivo which helps cells culture better, such environments can therefore ensure more accurate observations of cellular behavior in response to external stimuli [5]. However, microfluidic devices suffered from limited means to manipulate cells. In recent years, several methods have been used to immobilize cells within particular regions of the microfluidic channels, such as cell adhesion [6,7], within microwells [8–10], weir-type filters [11], and on a micromesh [12]. Photocrosslinked hydrogel polymers are an especially attractive matrix for cell immobilization within a microfluidic system due to their high water content, softness and mass transfer properties [13–16]. Moreover, cells can be selectively immobilized inside hydrogels with controlled shapes under different shapes of photomasks using a photolithography setup. Photocrosslinked hydrogels have previously been used to encapsulate several other biomaterials such as DNA [17,18], proteins [19], and enzymes [20,21] without suffering severe loss of enzyme activity. Hydrogel immobilization of biomaterials is effective because pores within the hydrogels are on the order of 1–10 nm in diameter [22–24], which is convenient for small molecules like cell culture nutrients and oxygen to penetrate into hydrogel microstructures. In our previous work, we fabricated

* Corresponding author. Tel.: +86 10 62792343; fax: +86 10 62792343.
E-mail address: jmlin@mail.tsinghua.edu.cn (J.-M. Lin).

0003-2670/$ – see front matter © 2010 Elsevier B.V. All rights reserved.
doi:10.1016/j.aca.2010.03.015

poly(ethylene glycol) (PEG) hydrogel microarrays to encapsulate DNA and mammalian cells using photopolymerization for bioassays [18].

In this paper, we described the fabrication of hydrogel microstructures containing cells in microfluidic channels for anticancer drug analysis. Hydrogel microstructures with controlled morphology and position on the microfluidic devices were generated using a photolithography setup without using photomasks. It provided a conventional way to selective encapsulation of multiple cells for bioassays. Before conducting stimulation experiments on hydrogel encapsulated human liver carcinoma HepG2 cells and human lung epithelial A549 cells inside microchannels, the precursor composition and crosslinking parameters were investigated to evaluate the influence of cell viability inside photocrosslinked hydrogels. After the hydrogel encapsulated cells stimulated by two anticancer drugs, the intracellular glutathione (GSH) and reactive oxygen species (ROS) were detected by using two specific probes, 2,3-naphthalenedicarboxaldehyde (NDA) and dihydroethidium (DHE), respectively. In comparison to the similar experiments performed on 96-well plate, we demonstrated that the method of cells encapsulated inside hydrogels had advantages to selectively immobilize cells and provided a simple method for biomedical basic research and drug screening.

2. Experimental

2.1. Reagents and materials

Polydimethylsiloxane (PDMS) and curing agent were purchased from Dow Corning (Sylgard 184, Midland, MI, USA). Negative SU-8 photoresist (SU-8 2050) and developer were obtained from MicroChem (Newton, MA). Pyrex wafers of 3 in. were purchased from SCHOTT Guinchard (Yverdon, Switzerland). 3-(Trichlorosilyl) propyl methacrylate (TPM) for surface modification was obtained from Fluka Chemicals (Milwaukee, WI). Poly(ethylene glycol) diacrylate (PEGDA, 700 MW, Sigma) and two kinds of photoinitiators, 2-hydroxy-2-methylpropiophenone (HMPP, Sigma) and 2-hydroxy-1-(4-(hydroxyethoxy) phenyl)-2-methyl-1-propanone (Irgacure 2959, HPMP, CIBA Chemicals) were used to encapsulate cells. N-vinyl pyrrolidone (NVP) which used to dissolve HPMP was purchased from Aldrich Chemical Co. (Milwaukee, WI). Live/Dead assay kit for mammalian cells was purchased from Invitrogen (CA, USA). Actinomycin D (Act D, Beyotime Institute of Biotechnology Co., China) and methotrexate (MTX, Fluka Chemicals) were used as model drugs to screen the cytotoxicity against HepG2 and A549 cells. Two specific fluorescence probes, NDA (Tokyo Kasei Kogyo Co., Japan) and DHE (Beyotime Institute of Biotechnology Co., China) were used to identify the variations of cellular GSH and ROS after exposure to anticancer drugs.

2.2. Microfluidic device fabrication

In all our experiments, we used straight microchannels with a height of 50 μm, a width of 1 mm and a length of 1 cm for cell-based assays. The microfluidic device was fabricated from PDMS using standard softlithography and replica molding techniques [25]. Briefly, a SU-8 2050 negative photoresist was spin-coated on a silicon wafer at 3000 rpm to obtain a 50 μm thick layer. After photolithographic patterning of a photoresist coated silicon wafer, a mold that carried a relief of the desired microstructure was generated. A 10:1 weight mixture of PDMS prepolymer and curing agent was stirred thoroughly and then degassed under vacuum. The polymer mixture was poured onto the master and baked in an oven at 80 °C for 2 h. After curing, the PDMS replica was peeled off from the master and the connection holes were punched using a syringe needle. Then the PDMS was irreversibly sealed with a glass slide after oxygen plasma treatment (PDC-32G, Harrick Plasma, Ithaca, NY, USA) for 90 s, and then baked overnight at 60 °C.

2.3. Cell culture

HepG2 and A549 cells were cultured in Dulbecco's Modified Eagle's Media (DMEM; Gibco, Grand Island, NY) containing 100 μg mL^{-1} penicillin, 100 μg mL^{-1} streptomycin and 10% fetal bovine serum. Cells were kept at 37 °C in 5% CO_2-humidified air atmosphere and passaged every two or three days at a subculture ratio of 1:5. For encapsulation experiments, cells were trypsinized with 0.25% (w/v) trypsin and released from 60 cm^2 polystyrene tissue culture flasks into suspension. The cell viability was determined by Live/Dead assay kit.

2.4. Fabrication hydrogel encapsulated cell arrays

Before fabricating hydrogel microstructures containing cells, the inner surfaces of the microchannels were modified with TPM monolayer to enhance the adhesion between hydrogel micropatches and glass surfaces [26]. Cell suspension was centrifuged at 1000 rpm for 5 min and resuspended in phosphate buffer solution (PBS), and then mixed with PEGDA precursor solution containing 0.5% photoinitiator. In this study, we used two common photoinitiators, HMPP and HPMP, and the photopolymerization conditions by using these two photoinitiators were investigated. The hydrogel precursor solution containing HepG2 cells was infused into the microchannels which were already treated with TPM. The UV light beam (wavelength 340–380 nm) of a fluorescence microscope (Leica DMI 4000 B, Wetzlar, Germany) was manually focused on the desired cells and induced the photopolymerization of the PEGDA precursor to generate hydrogel micropatch arrays with cylindrical shapes. The remaining unreacted hydrogel precursor and cells were removed using PBS. To add additional cell types, prepolymer solution containing A549 cells was then injected into the channels and exposured to UV light to form additional cell-laden hydrogel microstructure arrays with rectangular shapes. The process for the formation of cell arrays inside hydrogel microstructures was illustrated in Fig. 1A–C.

2.5. Cell viability assays

A mammalian cell Live/Dead assay kit composed of 2 μM calcein AM and 4 μM ethidium homodimer-1 (EthD-1) was used to investigate the viability of hydrogel encapsulated cells in the microfluidic devices. The nonfluorescent cell-permeant calcein AM can well retain within live cells, producing an intense uniform green fluorescence under intracellular esterase action. While EthD-1 can enter cells with damaged membranes and produce a bright red fluorescence by binding to nucleic acids in dead cells. For this assay, 0.5 μL of calcein AM and 2 μL of EthD-1 were added to 1 mL PBS to prepare the staining solution. After encapsulation of cells inside hydrogel microstructures in the microchannels, the staining solution was introduced for 30 min incubation at room temperature. Then fresh PBS was injected into the microchannels at a flow rate of 10 μL min^{-1} for 5 min to wash away the excess dyes. The images of the entrapped cells were observed under an inverted fluorescence microscope (excitation, 450–490 nm; emission, 515–550 nm) and analyzed. In order to assess the potential of long-term viability of cells in hydrogels, cell culture medium was then introduced into the microchannels at a flow rate of 5–50 μL min^{-1} with a syringe pump (Harvard, PHD 2000) for the culture of the encapsulated cells inside the microfluidic devices. The microfluidic devices were then placed into a Petri dish and incubated at 37 °C in 5% CO_2-humidified air atmosphere prior for further examination. The cell culture medium

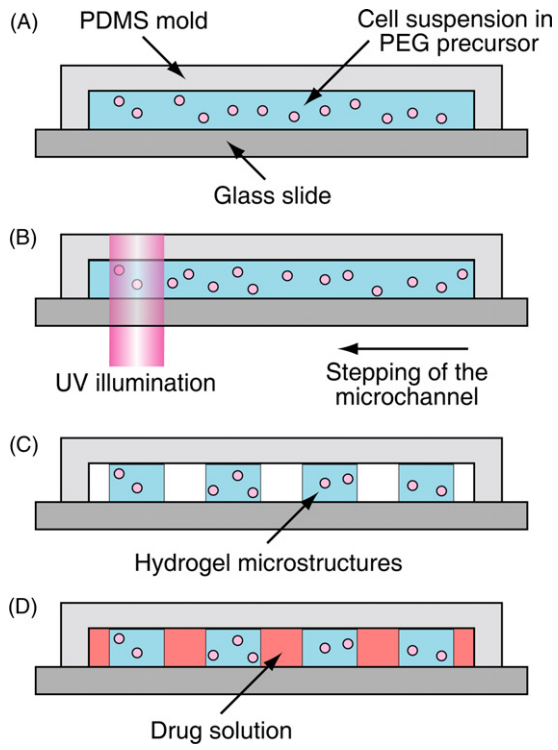

Fig. 1. Schematic diagram of the process for the formation of hydrogel microstructures containing living cells by photopolymerization and the application on drug analysis. (A) Cell suspension in hydrogel precursors was injected into the microchannels. (B) Array of hydrogel encapsulated cells was formed by in situ UV photopolymerization using a fluorescence microscope. (C) The remaining unreacted hydrogel precursor was washed away by PBS. (D) Drugs were injected into the channels to incubate with hydrogel encapsulated cells.

in the microchips was replaced with fresh medium everyday to supply enough nutrients and to wash away the cellular waste. The viability of the hydrogel encapsulated cells was tested with the Live/Dead assay kit everyday.

2.6. Determination of GSH and ROS in hydrogel encapsulated cells

Anticancer drugs, Act D and MTX, were used as model drugs to induce cell apoptosis, and the contents of cellular GSH and ROS were measured after exposure to anticancer drugs with different concentrations. Since GSH and ROS are natively nonfluorescent, we used two specific fluorescence probes NDA and DHE to label the intracellular GSH and ROS that their derivation can be detected by fluorescence microscope. The nonfluorescent NDA is able to bind with GSH to form green fluorescent product, while nonfluorescent DHE can be converted to red fluorescent ethidium by intracellular ROS. The fluorescence intensities of ethidium and GSH–NDA adduct were directly proportional to the intracellular contents of ROS and GSH by image analysis.

Prior to cell apoptosis experiments, the cytotoxicity of the two drugs on HepG2 and A549 cells were performed on 96-well plate. IC_{50} of the two drugs were below 5 μM, while the degrees of the cytotoxicity were different. Stock solutions of test compounds were serially diluted in medium to obtain the desired final concentrations. After encapsulation of HepG2 and A549 cells inside hydrogel microstructures, different concentrations of Act D and MTX were injected into the microchannels for 24 h incubation in CO_2 incubator (Fig. 1D). A mixture of 10 μM NDA and 25 μM DHE was then introduced into the microchannels and incubated at 37 °C for 30 min. PBS was then introduced into the microchannels to wash away unreacted NDA and DHE. Fluorescence images were acquired by using a fluorescence microscope equipped with a cooled CCD camera with software of Leica Application Suite, LAS V2.7. Image analyses were performed using commercially available image analysis software (QCapture Pro, Version 5.1.1.14, Media Cybernetics, USA).

3. Results and discussion

3.1. Fabrication of multiphenotype cell microarrays

The traditional methods for the size controlling of the photopolymerized hydrogel microstructures containing cells typically needed to use photomasks. In our method, a field diaphragm offered by fluorescence microscope was used to control the UV illumination region, by which the morphology of hydrogel microstructures can be easily regulated, such as cylindrical and rectangular shapes. The sizes of the microstructures were controlled by the magnification of objective and field diaphragm of the fluorescence microscope. Using the lithography setup, the spatial resolution on the position of hydrogel microstructures can be controlled in micrometers, and the dimensional accuracy of the hydrogel microstructure fabrication was in 30 μm. The UV source is an external 75 W xenon lamp, and the UV intensity can be adjusted by the power of the lamp. In the hydrogel photopolymerization, the maximum power was used. The objective with magnification of 20× was used for photopolymerization in our experiments. By using this fluorescence microscope, cells could be selectively, precisely and flexibly immobilized in the microchannels. The method offered several advantages as follows: firstly, it was capable to immobilize cells at a certain place for long-term observation that cannot be realized by conventional methods; secondly, it was possible to encapsulate different phenotypes of cells on a same array; thirdly, the microenvironments for cell culture inside the microchannels could be precise controlled, ensuring the reliable results from the experiment. As shown in Fig. 2, HepG2 and A549 cells were encapsulated inside arrays with different shapes of hydrogel microstructures in the same microchannel. HepG2 cells were encapsulated inside cylindrical hydrogel microstructures (78 μm × 78 μm × 50 μm), while A549 cells were encapsulated inside rectangular hydrogel microstructures (330 μm × 217 μm × 50 μm). The number of cells encapsulated inside hydrogel microstructures can be controlled by the cell density in PEGDA precursor solution. Before injecting the cell-containing hydrogel precursor solutions, the surfaces of the channels were chemical modified with TPM. After this treatment, the photopolymerized hydrogel microstructures were not detached from glass surfaces even under relatively high flow rate (up to 100 μL min^{-1}). Thus, the hydrogel encapsulated cells can be accurately immobilized in the microchannels for long-term investigation. Besides, the height of the hydrogel microstructures can also be controlled by the depth of the microchannels. The height of hydrogel microstructures is generally about 2 μm lower than the depth of the microchannels due to the inhibition on photopolymerization caused by the higher concentration of oxygen nearby the inner surface of PDMS [27].

3.2. Viability of encapsulated cells

The transparent hydrogel microstructures are amenable to imaging and detection via bright field and fluorescence microscopy, when the hydrogel slab is held on a transparent chamber slide. The cell viability was assessed by Live/Dead assay kit. Several researches have shown that the parameters of monomer, photoinitiator concentrations, and polymerization time have significant influence on cell viability inside photocrosslinked hydrogels [28,29]. The goal of

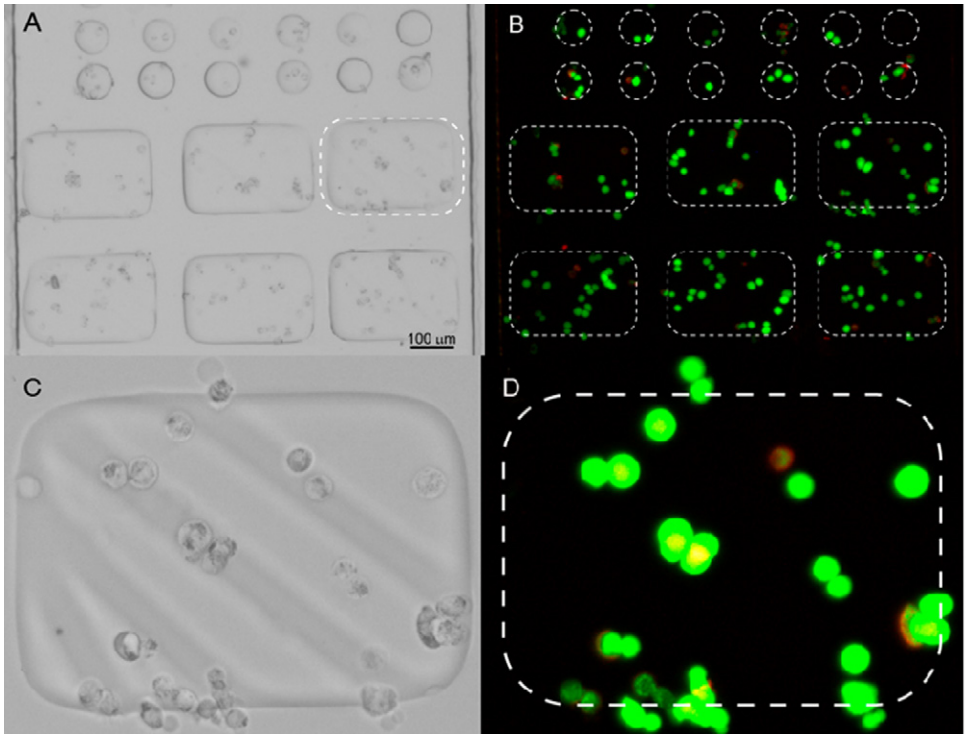

Fig. 2. (A) Optical image of hydrogel microstructure arrays containing two phenotypes cells: HepG2 and A549 cells. HepG2 cells were encapsulated inside cylindrical hydrogel microstructures (78 μm × 78 μm × 50 μm), while A549 cells were encapsulated inside rectangular hydrogel microstructures (330 μm × 217 μm × 50 μm). (B) Corresponding fluorescence image for the cell viability expressed by Live/Dead assay kit (live cells, green). (C and D) Enlarged optical and fluorescence images of one array element.

our work was to obtain maximum cell viability in the hydrogels by optimizing the prepolymer composition and photocrosslinking conditions for cell analysis. Because the parameters for the generation of hydrogel microstructures are not the same for different polymers and photoinitiators, we need to optimize them experimentally. Although hydrogel microstructures can be formed under a certain length of UV exposure time, it is better to shorten the UV exposure time for a certain concentration of PEGDA and photoinitiator with regular formed hydrogel and maximized cell viability. The optimum UV exposure of the prepolymer solutions can produce well-shaped hydrogel microstructures, while underexposure or overexposure would lead to distortion in their shapes and may influence the cell viability seriously. The cell viability and exposure time were compared by using precursor solutions containing two common photoinitiators, HMPP and HPMP with the same concentration. It took less than 2 s for UV exposure of polymer solution containing HMPP to form hydrogel microstructures, much shorter than the prepolymer solution containing HPMP (20 s) to achieve the same cell viability (data not shown). Hence, we finally selected HMPP as the photoinitiator to generate hydrogels. A549 cells were used as a model to study the effect of UV exposure time on the shapes of hydrogel microstructures and the corresponding cell viability, and the results were presented in Table 1. With the increasing UV exposure time, the cell viability decreased at each volume ratio

Table 1
The effect of UV exposure time on the viability of A549 cells.

Volume ratio of cell suspension to PEGDA precursor	UV exposure time (ms)	Cell viability (%)	The shape of hydrogel microstructure
1/1	100	86.5 ± 7.8	△
	200	75.8 ± 7.5	□
	300	69.8 ± 8.2	△
2/1	300	88.0 ± 8.4	△
	400	82.4 ± 6.9	□
	500	82.3 ± 5.8	△
3/1	700	89.6 ± 8.5	△
	800	86.2 ± 8.2	□
	900	76.2 ± 7.3	△
4/1	1100	100.0 ± 0	△
	1200	97.2 ± 4.0	□
	1300	94.1 ± 4.9	△
5/1	1400	100.0 ± 0	△
	1500	99.6 ± 0.9	□
	1600	95.0 ± 6.9	△

□: well-shaped hydrogel microstructure. △: distorted hydrogel microstructure.

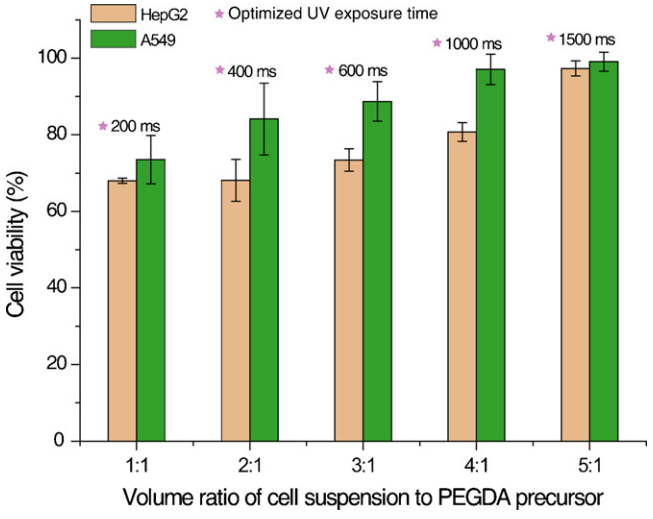

Fig. 3. The viabilities of HepG2 and A549 cells and optimized UV exposure times at different volume ratio of cell suspension to PEGDA precursor containing 0.5% HMPP initiator. The optimized exposure times were marked above the corresponding conditions in the histogram.

of cell suspension to PEGDA precursor with 0.5% photoinitiator (from 1/1 to 5/1). At each volume ratio, the shapes of hydrogel microstructures can be formed well only at the second UV exposure time. Under the optimized UV exposure time, the viabilities of HepG2 and A549 cells at different volume ratios were shown in Fig. 3. Viabilities of the two phenotypes both increased with the increasing volume ratio and viability of A549 cells was about 20% higher than HepG2 cells when the volume ratio was below 4/1, it is indicated that A549 cells have higher physiological activity than HepG2 cells in hydrogel precursor solution. However, the viabilities of two cells were nearly 100% at the volume ratio of 5/1. Cell viabilities at the volume ratio of 4/1 and 5/1 were high (>80%), but the exposure time required to crosslink the hydrogels was also increased (>1000 ms) because of the decreasing concentrations of PEGDA and photoinitiator in precursor solutions.

In order to perform cell-based assays on hydrogel encapsulated cells in the microchannels, it is necessary to keep their long-term viability. HepG2 and A549 cells at a density of 1×10^6 cells mL^{-1}, encapsulated inside hydrogel microstructures, were cultured in the microfluidic device and their viabilities were investigated for a few days. It is well-known that PDMS is nontoxic to various cell types and the permeability to O_2 and CO_2 is very excellent [30]. Consequently, the PDMS microfluidic device was very appropriate for cell culture and cell-based assays. The hydrogel encapsulated cells were cultured in 5% CO_2 and 95% air at 37 °C, and their viabilities were monitored by fluorescence microscope equipped with CCD camera for five days. During the long-term culture, the culture medium in the microchannels was prone to evaporate due to the permeability of PDMS. In order to solve this problem, the upper surfaces of microfluidic devices were covered with culture medium to prevent the evaporation of cell culture medium from the microchannels.

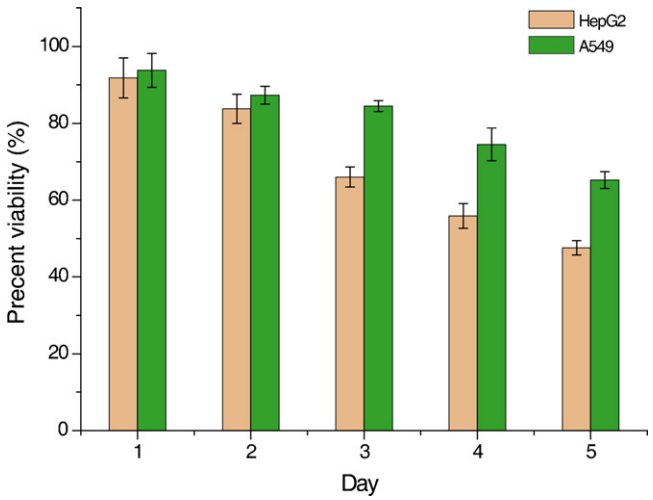

Fig. 4. Viability of encapsulated cells for long-term culture inside microchannels. The HepG2 and A549 cells were encapsulated inside hydrogel microstructures and incubated in a 95% air/5% CO_2-humidified incubator at 37 °C for five days. Viabilities were evaluated by Live/Dead assay kit every day.

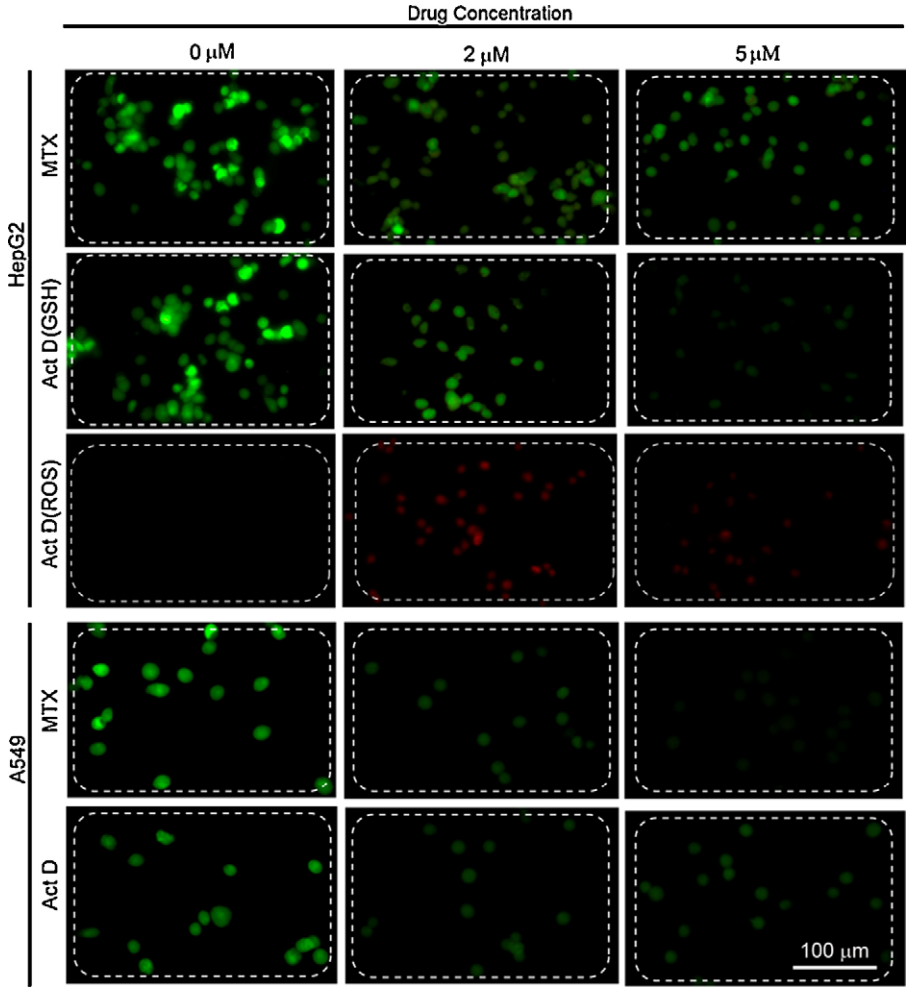

Fig. 5. Fluorescence images associated with parameter of GSH in HepG2 and A549 cells after exposure to anticancer drugs, and the parameter of ROS in HepG2 cells after stimulated by Act D. Cells were treated with different concentrations of MTX and Act D for 24 h and imaged by fluorescence microscope at a magnification of 20×.

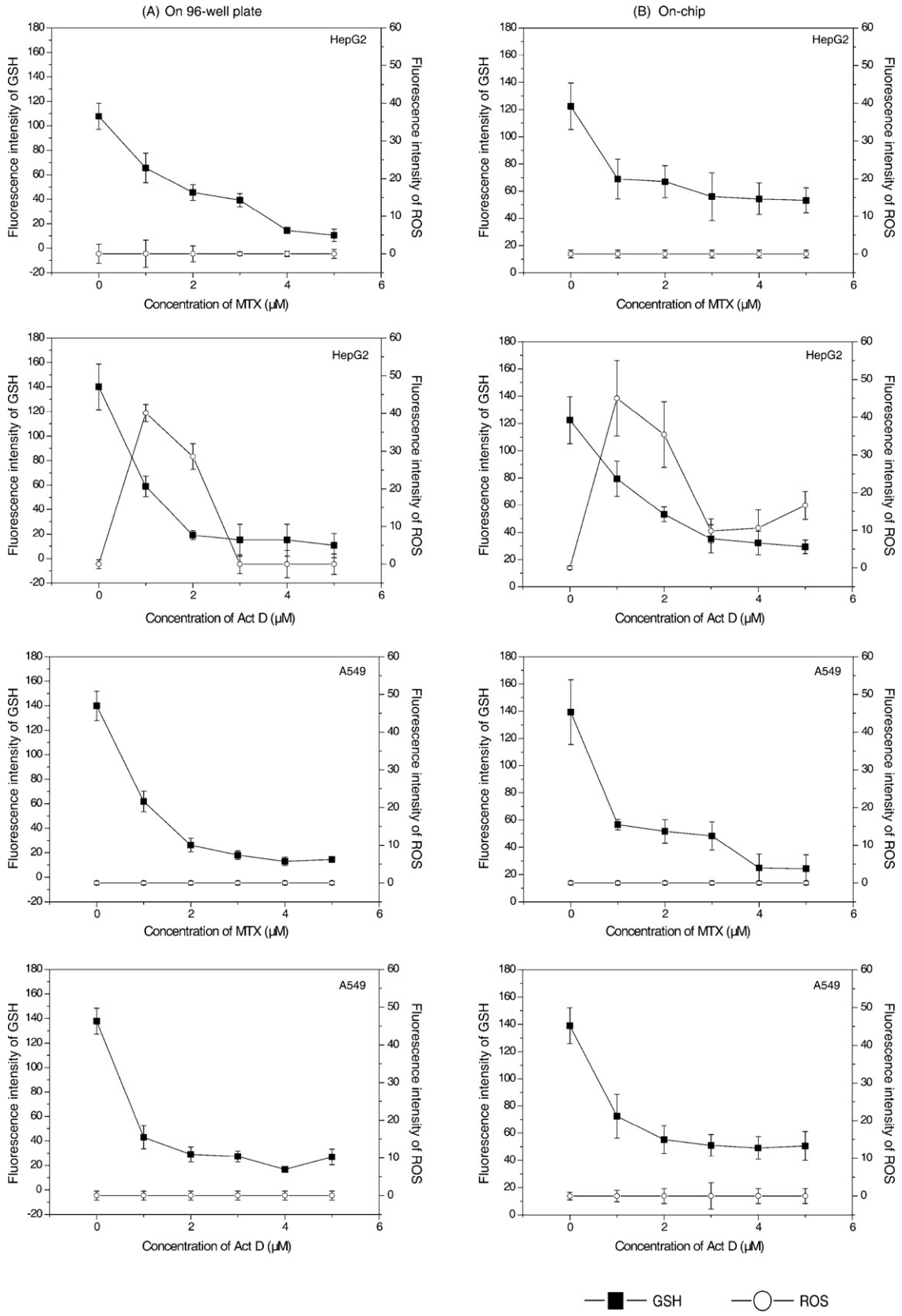

Fig. 6. Plots of two anticancer drugs for the parameters of GSH and ROS as normalized fluorescence intensity per cell. HepG2 cells (A and B) and A549 cells (C and D) were treated with varying concentrations of MTX and Act D for 24 h. The standard error bars means the variation of three independent experiments.

Additionally, pipette tips were inserted into the inlets and outlets of the microchannels to avoid the dilution of anticancer drugs by the diffusion of the culture medium into the microchannels. With this treatment, no evaporation was observed from the microchannels for several days. As shown in Fig. 4, the viabilities of HepG2 and A549 cells decreased over the incubation period, but the viability of A549 cells was a little higher than HepG2 cells. About 70% of encapsulated A549 cells kept their viability within five days, while about 65% HepG2 cells maintained their viability for three days. It is indicated that both cells can be used for chemical stimulation and chemical toxicity assays, and the process only need to be treated for one or two days.

3.3. Simultaneous determination of intracellular GSH and ROS in HepG2 and A549 cells

For cell apoptosis assay, a microfluidic device consisted of several parallel straight channels was used. Different concentrations of drugs can be used to stimulate the encapsulated cells inside different channels, which hold great promise for the cell-based high-throughput assays. Taking advantage of the encapsulation of cells within hydrogels, drugs with small molecule weight can be selectively contact with cells to reduce the interference of chemicals around. The majority of anticancer drugs have molecule weight less than 1000 that can easily permeate into the hydrogels. GSH and ROS are two important redox parameters related to apoptosis and oxidative stress which are considered as cellular signaling molecules in response to various extracellular stimulations. GSH is the major intracellular thiol-containing compound, existing mainly in its reduced form under steady-state conditions [31]. ROS which is widely generated during aerobic metabolism in biological systems are found to damage cellular unsaturated lipids, proteins and DNA. Owing to the biological and clinical significance, simultaneous determination of intracellular GSH and ROS and monitoring of variations of GSH and ROS levels in response to chemical stimulations are benefit for clinical diagnosis at early stages of a disease.

Due to the size of rectangular hydrogel microstructures is three times larger than that of cylindrical, the number of cells encapsulated inside two shapes of hydrogels may have great difference. In order to keep nearly the same cell number, two phenotypes of cells were finally encapsulated inside rectangular hydrogel microstructures for the following anticancer drug analysis. In addition, to assess whether hydrogel encapsulation method had any effect on the cellular redox state, anticancer drugs stimulation on HepG2 and A549 cells were first performed on 96-well plate. By comparison, it is found that intracellular GSH and ROS have the similar variation trends, as shown in Fig. 6. The variations of intracellular GSH and ROS in hydrogel encapsulated cells were further characterized after stimulated by anticancer drugs with the concentration of 0–5 μM for 24 h. Intracellular GSH of HepG2 and A549 cells had different degrees of variations after the treatment of MTX and Act D, but intracellular ROS varied only in HepG2 cells after treated with Act D. Fig. 5 shows the representative fluorescence images for GSH in two phenotypes of cells after stimulated by two anticancer drugs and ROS in HepG2 cells after Act D treatment. With the increasing concentrations of MTX and Act D, intracellular GSH had different degrees of depletion in the two phenotypes. It is indicated that the intracellular redox balance was disturbed to different degrees in anticancer drug-induced apoptosis of HepG2 and A549 cells. The quantitative results of drug stimulation experiments at various concentrations related to two parameters were shown in Fig. 6B. The results showed that the levels of GSH and ROS in HepG2 and A549 cells were differently influenced by MTX and Act D compounds at the tested concentration range after 24 h treatment. Act D caused obvious generation of ROS in HepG2 cells at the concentration of 1 μM, while inducing the depletion of two compounds at higher concentration and only generating a small quantity of ROS. Among the results, MTX and Act D exhibited indistinct effects on intracellular redox states in two phenotypes of cells, demonstrating the selectivity of these drugs on the disturbance of redox balance within different cells.

4. Conclusions

We fabricated PEG hydrogel microstructures with controlled morphology and position to encapsulate mammalian cells inside microchannels with a simple and inexpensive photolithography technique which is beneficial for cell-based assays. Different phenotypes of cells can be simultaneously immobilized inside three-dimensional hydrogel microstructures on a same array with different morphologies for identity. The experimental parameters (UV exposure time, photoinitiator and PEGDA concentrations) for encapsulation of cells inside hydrogels using a photolithography setup were characterized to obtain the maximum cell viability. More than 90% of cells encapsulated within the optimized prepolymer solutions remained viable. Furthermore, hydrogel encapsulated cells were successfully cultured inside microfluidic devices, and the cells maintained their viability for at least three days. The encapsulated cells were used to perform anticancer stimulation, and intracellular GSH and ROS with regard to apoptosis were detected by two specific fluorescent probes. By comparison of quantitative analysis of intracellular GSH and ROS contents between the cells encapsulated inside hydrogels and cultured on 96-well plate, it is demonstrated that this simple method for selective encapsulation of single cells inside hydrogel microstructures in ordinary laboratory is very useful for biomedical basic research and drug screening.

Acknowledgements

This work was supported by the National Natural Science Foundation of China (No. 20935002) and National Basic Research Program of China (973 Program, No. 2007CB714507).

References

[1] D. Wlodkowic, J. Skommer, Z. Darzynkiewicz, Cytometry Part A 73A (2008) 496–507.
[2] Z. Darzynkiewicz, G. Juan, X. Li, W. Gorczyca, T. Murakami, F. Traganos, Cytometry 27 (1997) 1–20.
[3] J.M. Brown, L.D. Attardi, Nat. Rev. Cancer 5 (2005) 231–237.
[4] T. Vilkner, D. Janasek, A. Manz, Anal. Chem. 76 (2004) 3373–3385.
[5] J.C. McDonald, D.C. Duffy, J.R. Anderson, D.T. Chiu, H. Wu, O.J. Schueller, G.M. Whitesides, Electrophoresis 21 (2000) 27–40.
[6] K. Jo, M.L. Heien, L.B. Thompson, M. Zhong, R.G. Nuzzo, J.V. Sweedler, Lab Chip 7 (2007) 1454–1460.
[7] H. Hufnagel, A. Huebner, C. Gulch, K. Guse, C. Abell, F. Hollfelder, Lab Chip 9 (2009) 1576–1582.
[8] A.R. Wheeler, W.R. Throndset, R.J. Whelan, A.M. Leach, R.N. Zare, Y.H. Liao, K. Farrell, I.D. Manger, A. Daridon, Anal. Chem. 75 (2003) 3581–3586.
[9] A. Khademhosseini, J. Yeh, S. Jon, G. Eng, K.Y. Suh, J.A. Burdick, R. Langer, Lab Chip 4 (2004) 425–430.
[10] Y. Sasuga, T. Iwasawa, K. Terada, Y. Oe, H. Sorimachi, O. Ohara, Y. Harada, Anal. Chem. 80 (2008) 9141–9149.
[11] D. Di Carlo, N. Aghdam, L.P. Lee, Anal. Chem. 78 (2006) 4925–4930.
[12] T. Matsunaga, M. Hosokawa, A. Arakaki, T. Taguchi, T. Mori, T. Tanaka, H. Takeyama, Anal. Chem. 80 (2008) 5139–5145.
[13] W.G. Koh, L.J. Itle, M.V. Pishko, Anal. Chem. 75 (2003) 5783–5789.
[14] P. Panda, S. Ali, E. Lo, B.G. Chung, T.A. Hatton, A. Khademhosseini, P.S. Doyle, Lab Chip 8 (2008) 1056–1061.
[15] D.R. Albrecht, V.L. Tsang, R.L. Sah, S.N. Bhatia, Lab Chip 5 (2005) 111–118.
[16] Y. Ling, J. Rubin, Y. Deng, C. Huang, U. Demirci, J.M. Karp, A. Khademhosseini, Lab Chip 7 (2007) 756–762.
[17] K.G. Olsen, D.J. Ross, M.J. Tarlov, Anal. Chem. 74 (2002) 1436–1441.
[18] J.J. Liu, D. Gao, H.F. Li, J.M. Lin, Lab Chip 9 (2009) 1301–1305.
[19] W. Lee, D. Choi, J.H. Kim, W.G. Koh, Biomed. Microdevices 10 (2008) 813–822.
[20] W. Zhan, G.H. Seong, R.M. Crooks, Anal. Chem. 74 (2002) 4647–4652.
[21] J.C. Zguris, L.J. Itle, D. Hayes, M.V. Pishko, Biomed. Microdevices 7 (2005) 117–125.
[22] G.M. Cruise, D.S. Scharp, J.A. Hubbell, Biomaterials 19 (1998) 1287–1294.

[23] R.A. Scott, N.A. Peppas, Biomaterials 20 (1999) 1371–1380.
[24] M.B. Mellott, K. Searcy, M.V. Pishko, Biomaterials 22 (2001) 929–941.
[25] M.A. Unger, H.P. Chou, T. Thorsen, A. Scherer, S.R. Quake, Science 288 (2000) 113–116.
[26] G.H. Seong, W. Zhan, R.M. Crooks, Anal. Chem. 74 (2002) 3372–3377.
[27] D. Dendukuri, P. Panda, R. Haghgooie, J.M. Kim, T.A. Hatton, P.S. Doyle, Macromolecules 41 (2008) 8547–8556.
[28] S.J. Bryant, C.R. Nuttelman, K.S. Anseth, J. Biomater. Sci: Polym. E 11 (2000) 439–457.
[29] A. Revzin, R.J. Russell, V.K. Yadavalli, W.G. Koh, C. Deister, D.D. Hile, M.B. Mellott, M.V. Pishko, Langmuir 17 (2001) 5440–5447.
[30] S.G. Charati, S.A. Stern, Macromolecules 31 (1998) 5529–5535.
[31] K. Davison, S. Cote, S. Mader, W.H. Miller, Leukemia 17 (2003) 931–940.